Magnetic profile and interlayer exchange coupling in fcc Fe$_n$/Ni$_m$ (001) superlattices

A. Hadj-Larbi and S. Bouarab

Laboratoire de Physique et Chimie Quantique, Faculté des Sciences, Université Mouloud Mammeri, 15000 Tizi–Ouzou, Algeria

C. Demangeat

Institut de Physique et de Chimie des Matériaux de Strasbourg, 23, rue du Loess, F-67037 Strasbourg, France

We have performed *ab initio* calculations to study the electronic and magnetic structures of fcc Fe$_n$/Ni$_m$(001) superlattices. A ferromagnetic coupling between Fe and Ni atoms is always obtained at the interfaces for any value of m or n. The interlayer exchange coupling between adjacent Ni$_m$ slabs through Fe$_n$ spacer displays an oscillatory behavior which is strongly modified when mixed Fe-Ni interfaces are considered. The iron atoms close to the interface form an induced ferromagnetic arrangement whereas the atoms inside the fcc Fe film give rise to an antiferromagnetic order. The compositional ordering at the Fe/Ni interface introduces a $c(2 \times 2)$ type of antiferromagnetism in the Fe layers in the case of ferromagnetic interlayer exchange coupling.

I. INTRODUCTION

The fcc Fe/Ni superlattice is a very peculiar system related to the magnetic instability of the γ-Fe and the ferromagnetic-induced polarization effect by the Ni slab on Fe atoms which depends on the local ordering. Of particular interest is the complexity of the interaction between the magnetic and compositional ordering. Recently, much attention has been addressed to this system by various experimental groups.

Lu *et al.*[1] have studied the epitaxial growth of γ-Fe on Ni (001) at room temperature with low-energy electron diffraction (LEED) and Auger electron spectroscopy. Their experiments indicate that Fe grows on the Ni (001) in a strained fcc structure, but films thicker than about six layers contain domains of the stable bcc phase. With a primary-beam diffraction-modulated electron emission (PDMEE) and secondary electron imaging techniques, Gazzadi *et al.*[2] predicted that for Fe films on a Ni(001) substrate the transition to the bcc phase occurs through nucleation of bcc(110) domains with the bcc[111]∥fcc[110] orientation. In Ni/Fe/Ni(111) trilayers, Fratucello *et al.*[3] measured, by Mössbauer spectroscopy, a high hyperfine field ($\approx$28 T) assigned to Fe atoms close to Fe-Ni interface with a high-spin ferromagnetic state and a low hyperfine ($\approx$8 T) field corresponding to inside Fe atoms with a low-spin antiferromagnetic state.

Edelstein *et al.*[4] have measured with a superconducting quantum interference device (SQUID) magnetometer a strong magnetic coupling between the Ni and Fe layers at the interface which enhances the magnetization of both Fe and Ni atoms. By using x-ray diffraction, Kuch and Parkin[5] have studied the structure of the Fe spacer in the Fe/Ni(001) multilayers. They show that, as the Fe layer thickness is increased, its structure varies from a vertically expanded fcc structure ($<$7 Å) to a nearly relaxed fcc phase ($<$14 Å), and finally to a bcc (011) phase. These three phases are respectively ferromagnetic, antiferromagnetic, and ferromagnetic. Kuch *et al.*[6] have used a combination of photoelectron emission microscopy and magnetic circular dichroism in soft x-ray absorption (XMCD) to study the magnetic phase of Ni/Fe/Co/Cu(100). They obtained three magnetically different thickness regions of Fe with effective spin moments per atom of $2.5\mu_B$ (below 3.5 ML), $0.7\mu_B$ (3.5–11 ML), and $2.0\mu_B$ (above 11 ML). By LEED and XMCD, O'Brien and Tonner[7] found distinct magnetic phases for the growth of Fe film on Ni. For Fe coverages below 5 ML the films are ferromagnetic, and between 5 and 11 ML the films are nonmagnetic, but include a ferromagnetic live monolayer (ML) at the Ni/Fe interface.

By LEED and PDMEE, Luches *et al.*[8] obtained for thin Fe films grown on Ni(001) evidence of intermixing between Fe and Ni in the first 3 ML. At low temperature, Fratucello and Prandini[9] detected a strong diffusion, by Mössbauer spectroscopy, at the Fe/Ni interface interpreted in terms of the minimization of the strain energy. Acharya *et al.*[10] with conversion electron Mössbauer spectroscopy show a mixing at the interface of Fe/Ni multilayers. The experimental investigations of Luches *et al.*, Fratucello *et al.*, and Acharya *et al.*[8–10] display clear evidence of alloying at the interface, in agreement with the usual phase diagram[11] of Ni-Fe.

From all these experimental studies a relevant point of general agreement is a strong ferromagnetic Fe-Ni coupling at the interfaces which display alloyed crystalline structure. Different magnetic phases are also observed in the Fe spacer.

On the theoretical side, Rao *et al.*,[12] using a first-principles molecular approach, have determined the equilibrium geometry, binding energies, and magnetic properties of FeNi clusters. The equilibrium geometries found for (NiFe)$_n$ ($n=1,2,3,4$) clusters have a large number of FeNi bonds, and energetically preferable isomers are those where Fe-Ni bonds are maximized. All clusters are found to be ferromagnetic and the magnetic moments per atom of these clusters are almost insensitive to the specific geometry. In all cases, the atomic magnetic moment is higher than those obtained for Fe and Ni in their bulk form. Moreover, their values are almost constant: $3\mu_B$ for Fe and $1\mu_B$ for Ni.

The aim of the present work is to present an *ab initio* study of the magnetic properties of $Fe_n/Ni_m(001)$ superlattices for $n=1,2,3,4,5,6$ and $m=3,5$. We have used the tight-binding linear muffin-tin orbital in the atomic-sphere approximation (TB-LMTO-ASA). The generalized gradient approximation (GGA) is used for the exchange-correlation potential of the density-functional theory (DFT) because local density approximation (LDA) does not reproduce the ground state of bulk[13] Fe. However, it is known that nonspherical effects (completely missing from the ASA) are important to the GGA. Nevertheless, as discussed by M'Passi-Mabiala *et al.*[14] the GGA approach used within the ASA improves considerably the agreement with the experimental results in the case of a half Mn monolayer adsorbed on fcc Co(001). Indeed, both XMCD and magneto-optical Kerr effect (MOKE) results displayed a ferromagnetic coupling between Mn and Co whereas LDA calculations by Meza-Aguilar *et al.*[15] obtained an antiferromagnetic coupling. It is another reason to use the GGA.

First we determine the lattice parameters of bulk fcc Ni and fcc Fe by minimization of the total energy. The ground state of fcc Fe is antiferromagnetic with a lattice parameter $a_{Fe}=6.56$ a.u. and a magnetic moment of $1\mu_B$. Depending on the lattice parameter, metastable ferromagnetic states with high ($2.5\mu_B$) and low ($1.2\mu_B$) spin are also obtained in agreement with Moruzzi *et al.*[16] We expect that these metastable magnetic configurations could be stabilized by pseudomorphic growth on suitable substrates. Beside the in-plane ferromagnetic configuration of Fe we have, for completeness, also considered the in-plane antiferromagnetic configuration $c(2\times2)$. Moreover, at the Fe/Ni interfaces some interdiffusion could take place. We have modeled it via a monolayer containing both Fe and Ni in an $Fe_{0.5}Ni_{0.5}$-ordered way.

II. THEORETICAL MODEL AND BULK PROPERTIES OF IRON AND NICKEL

As stated previously, the calculations are performed using a scalar-relativistic version of the k-space TB-LMTO method[17,18] with the atomic-sphere approximation. This method is usually based on the LDA (Ref. 19) of the density-functional theory.[20,21] The lattice parameters and atomic magnetic moments of the Ni and Fe fcc bulk are calculated using LSDA and GGA by minimization of the total energy. The Langreth-Mehl-Hu[22] and Perdew-Wang[23] GGA functionals have been tested and finally the Langreth-Mehl-Hu functional was retained because it gave the best agreement for Fe with other calculations.[13,16,24–29] As shown in Fig. 1, our calculation versus lattice parameter of fcc Fe leads to one nonmagnetic configuration for $a_{Fe}<6.46$ a.u. and three phases: nonmagnetic (NM), antiferromagnetic (AF), and ferromagnetic (FM) with low ($\approx1.0\mu_B$) and high ($\approx2.5\mu_B$) spins for $a_{Fe}>6.46$ a.u. The AF phase is generally more stable than the NM and FM phases and the ground state is obtained for a lattice parameter of 6.56 a.u. and a magnetic moment of $1.0\mu_B$. Let us notice that fcc iron can only be stabilized at low temperature as thin films epitaxially grown on appropriate substrates. Using the LDA and Langreth-
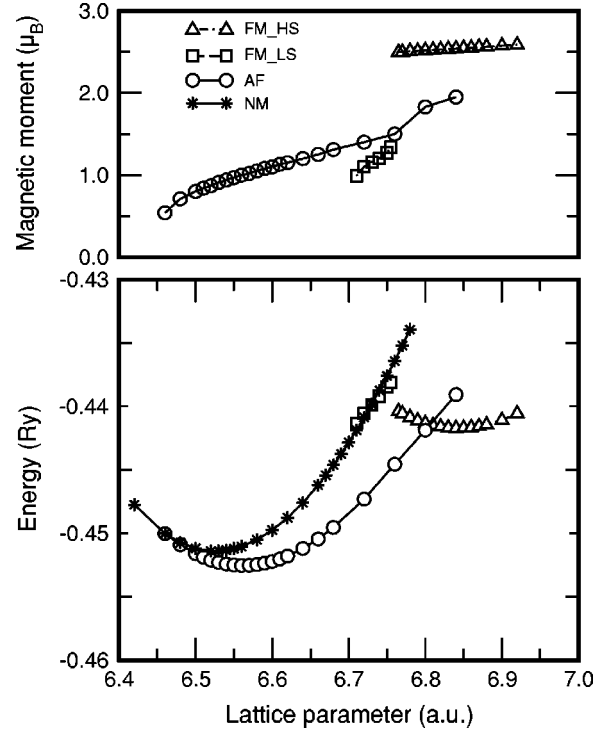

FIG. 1. Total energies (lower panel) and magnetic moments (upper panel) of fcc iron obtained from TB-LMTO-ASA calculations within the GGA for different magnetic orderings. Triangles indicate FM high spin; squares, FM low spin; stars, NM; and circles, AF order. The ground state is AF with $a_{Fe}=6.56$ a.u. and $\mu_{Fe}=1.0\mu_B$.

Mehl-Hu GGA the calculated lattice parameter for Ni is $a_{Ni}=6.61$ a.u. and the magnetic moment is $0.63\mu_B$. The Perdew-Wang GGA leads to $a_{Ni}=6.80$ a.u., higher than the experimental one (6.64 a.u.). In this context it is essential to note that there is significant difference between using the LDA or GGA. Although there exist different analytical forms for both approximations, there is nearly complete agreement about all the conditions that have to be satisfied by the corresponding analytical representations only in the case of the LDA. In spite of the very great success of the LDA to describe the properties of solids, this latter presents some deficiencies. The LDA leads to lattice constants which are in general underestimated (the case of α-Fe is well known) while cohesive energies and bulk moduli are correspondingly overestimated.

As there is still no such general agreement concerning the GGA, various functionals can lead to different results, as we have probed it in the present work for γ-Fe and Ni. The GGA Perdew-Wang functional yields an incorrect description of the magnetic structure of γ-Fe and overestimates the lattice parameter of Ni.

On the other side, it was already pointed out by Singh and Ashkenazi[30] that in the GGA, there is an increased tendency towards magnetism in general and, in particular, towards larger magnetic energies. Despite these deficiencies, the Langreth-Mehl-Hu GGA gives a good description of the magnetic structure for both fcc Fe and Ni elements contrary to the Perdew-Wang functional. The overestimation of the magnetic energy in the GGA used in the present work to

study the Ni_m/Fe_n multilayers is somewhat canceled in the calculation of the interlayer exchange coupling (IEC) which is defined as the total energy difference between the most stable magnetic arrangements of Fe atoms in the spacer layer for FM and AF spin orientations of two successive Ni_m slabs.

For all the Fe_n/Ni_m superlattices studied in the present paper we have considered pseudomorphic growth; i.e., the in-plane interatomic distance of Fe is chosen to be the same as that of fcc Ni, whereas the Fe-Fe out-of-plane interatomic distance is determined according to the constant volume approximation. However, we did not calculate the distance at the Ni-Fe interface because the ASA is known to yield incorrect results for energy changes that are connected to anisotropic deformation.[31] Instead, the Ni-Fe interface distance is chosen as the arithmetic mean value of the calculated Ni and Fe lattice parameters. In order to minimize the numerical errors we have considered in all calculations two atoms per plane and the antiferromagnetic supercell for both AF and FM interlayer exchange couplings investigated.

III. MAGNETIC MAP AND INTERLAYER EXCHANGE COUPLING OF Fe_N/Ni_M ($M=3,5$)

In this section we present the magnetic properties and the total energies of the Fe_n/Ni_3 and Fe_n/Ni_5 superlattices for $n=1,2,3,4,5,6$. We call the FM (AF) IEC the parallel (antiparallel) alignment of magnetic moments between two successive Ni_m slabs. We remember that the IEC is defined as the difference of the total energy between the most stable magnetic arrangements of Fe atoms in the spacer layers for FM and AF configurations of adjacent Ni_m slabs.

We notice also that since Fe atoms have larger moments than Ni, for any cases where we considered AF Ni-Fe coupling between next-nearest-neighbor atoms at the interface, we observe a spin flip of the Ni atom in order to have FM coupling with Fe. However, these magnetic configurations with AF Fe-Ni coupling at the interface are always found to be less stable.

After all these hypotheses, we investigate the following main points: (i) a possible dependence of the IEC versus the thickness of the Ni slabs by performing calculations of Fe_n/Ni_3 and Fe_n/Ni_5 for $n=1,2,3,4,5,6$; (ii) the Fe-Ni coupling at the interface; and (iii) the effect of Ni-Fe mixed interfaces on the stability, the magnetic map, and the IEC.

First, we discuss the magnetic maps of the Fe_n/Ni_3 (Fig. 2) and Fe_n/Ni_5 (Fig. 3) superlattices. Only the most stable solutions for ferromagnetic (left panels of Figs. 2 and 3) and antiferromagnetic (right panels) IEC's are reported. The magnetic moments on the Fe atoms at the interface with Ni are always enhanced as compared to the bulk fcc Fe. This enhancement depends on the Fe spacer thicknesses: it is $2.56\mu_B$ for $n=1$, $1.93\mu_B$ for $n=2$, $1.98\mu_B$ for $n=3,4$ and $1.95\mu_B$ for $n=5$. The magnetic moments of the Fe atoms decrease when their distance with the Ni slab increases. In the case of ferromagnetic IEC (Figs. 2 and 3), the most stable configurations display a ferromagnetic coupling between Fe and Ni at the interface. Moreover, for one and two Fe layers the superlattice remains totally ferromagnetic. If we start with a $c(2\times2)$ configuration for Fe as input the converged
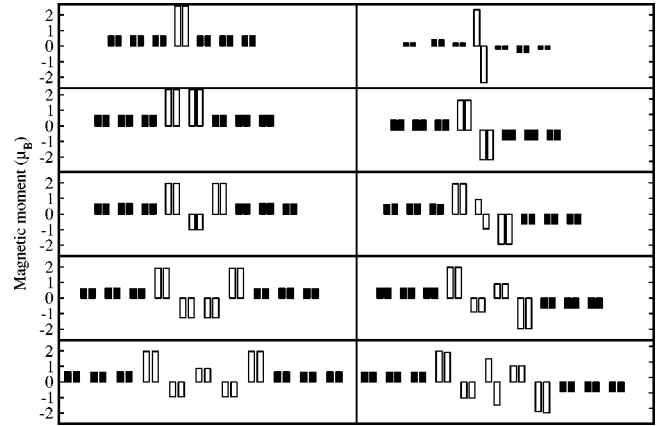

FIG. 2. Magnetic profiles (in μ_B) of Fe_n/Ni_3 ($n=1,2,3,4,5$) superlattices for FM and AF interlayer exchange couplings between Ni slabs (left and right panels, respectively). Dark (open) bars represent the values of the magnetic moments of the Ni (Fe) atoms. Two magnetically inequivalent atoms per plane have been considered.

solution turns out to be in-plane ferromagnetic. For $n>2$ and n odd the Fe monolayers tend to be antiferromagnetically coupled: the induced ferromagnetic polarization by the Ni atoms is destroyed by the intrinsic AF coupling present in bulk Fe.

In the case of an antiferromagnetic IEC (Figs. 2 and 3), besides the ferromagnetic Fe-Ni coupling which is always obtained at the interface, a $c(2\times2)$ solution in the central Fe plane is present for n odd. This $c(2\times2)$ magnetic configuration is necessary for a minimization of the spin frustration. A case worthy to discuss is Fe_1/Ni_3 and Fe_1/Ni_5 where the magnetic moments of the Ni atoms are very strongly depressed because of this $c(2\times2)$ solution in the Fe layer. For Fe_1/Ni_5 the magnetic moments of the interface Ni atoms are reduced by about 50% relatively to the bulk one ($0.63\mu_B$). A more drastic effect is seen for Fe_1/Ni_3 where the moments of the interface Ni atoms are strongly reduced ($0.07\mu_B$).
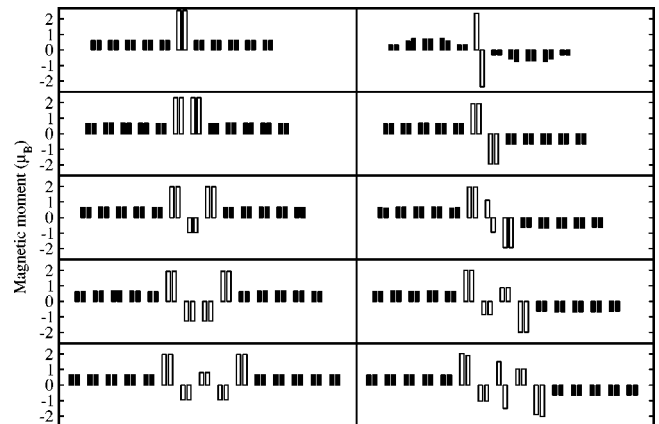

FIG. 3. Magnetic profiles (in μ_B) of Fe_n/Ni_5 ($n=1,2,3,4,5$) superlattices for FM and AF interlayer exchange couplings between Ni slabs (left and right panels, respectively); dark and open bars as in Fig. 2.
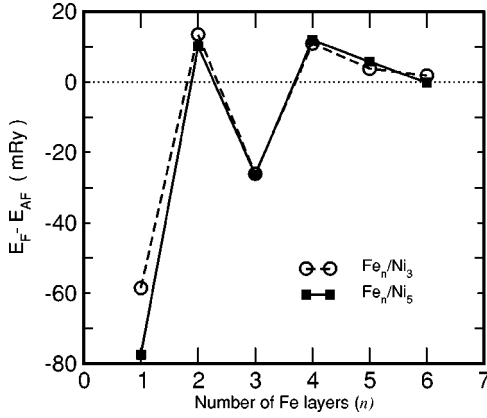
FIG. 4. The energy differences ($E_F - E_{AF}$) vs the number of Fe layers for Fe_n/Ni_3 (dashed line) and Fe_n/Ni_5 (solid line). E_F and E_{AF} are, respectively, the energy of the Fe_n/Ni_3 and Fe_n/Ni_5 superlattices in the case of a FM and AF interlayer exchange coupling between the Ni slabs.

Also, if as input for Fe_1/Ni_3 we choose a zero magnetic moment on Fe, after convergence we obtain a solution which is ferromagnetic IEC. This is not the case for Fe_1/Ni_5 where a zero magnetic moment on Fe remains; this magnetic configuration is, however, a metastable one. For n odd and $n > 2$, if we start with a zero magnetic moment on the central Fe layer in Fe_n/Ni_3 and Fe_n/Ni_5 superlattices, the converged (metastable) solution remains with that zero moment.

The difference of the total energies between ferromagnetic E_{FM} and antiferromagnetic E_{AF} configurations of adjacent Ni_m slabs is reported in Fig. 4 for Fe_n/Ni_3 (dashed line) and Fe_n/Ni_5 (solid line). We observe very similar behavior for both Ni thicknesses. The fcc Fe film mediates a decreasing oscillatory IEC up to $n = 4$, after which it remains of AF type for $n = 5$ and then disappears completely for $n = 6$.

IV. MIXED INTERFACES

Since Johnson *et al.*,[11] it has been well known that the Fe-Ni phase diagram shows that a stable alloy between Fe and Ni can be formed at any composition. Moreover, some authors[8-10,32] have explained their experiments via some kind of intermixing in the Fe/Ni superlattices.

Here we consider only the case of an ordered $Fe_{0.5}Ni_{0.5}$ interface of one layer thick. Different local atomic arrangements are considered depending on the number of iron layers (Fig. 5). If the number of Fe spacer layers is even (odd number of pure iron layers), two different cases of covering interface planes are distinguished: (i) a symmetric arrangement where one and the same type of atom occupies the same sublattice in both ordered $c(2 \times 2)$ magnetic interface layers [Fig. 5(a)] and (ii) an asymmetric arrangement in which one particular sublattice is occupied by the opposite type of atom in the two magnetic interfaces [Fig. 5(b)]. However, from energy point of view, these two atomic arrangements are found degenerated. The symmetric one appears more favored only by about 6 mRy.

In the case where the number of spacer layers is odd (even number of pure Fe layers) there is no distinction with
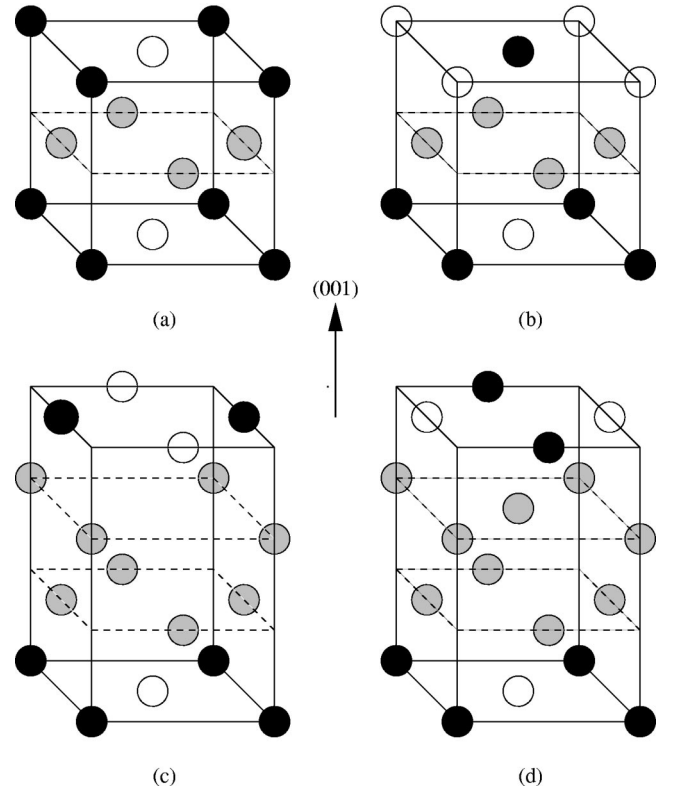

FIG. 5. Schematic view of the different atomic arrangements considered beyond the Ni-Fe interface: Fe layers (dashed lines, gray circles) and Ni-Fe magnetic layers (solid lines; Ni, solid circles; Fe, open circles) stacked along the (001) direction. For an odd number of Fe spacer layers the symmetric (a) and asymmetric (b) atomic arrangements are different. For an even number of Fe spacer layers, the two arrangements (c) and (d) are geometrically similar.

respect to an occupation of different sublattices with different types of atoms as they are geometrically equivalent [Figs. 5(c) and 5(d)].

In Table I we report the energy differences (δE) between the energies per supercell of the more stable states of the superlattices with perfect and $Fe_{0.5}Ni_{0.5}$-ordered interfaces versus the value of n [the number of Ni ($m = 5$) and Fe (n) atoms per supercell is the same in the two cases]. All the values reported in Table I are negative; i.e., the superlattices with a mixed interfaces are more stable than those with perfect interfaces for all the values of n. For this reason we discuss here the stability of the $Fe_{0.5}Ni_{0.5}$-ordered alloy, one monolayer thick, at the Fe/Ni interface and the effect of this interfacial mixing on the magnetic map of the multilayers. We focus, namely, on the spin polarization of fcc Fe and

TABLE I. The energy differences δE (mRy) between the superlattices Fe_n/Ni_5 with mixed layers at the interfaces and perfect interfaces for $n = 1,2,3,4,5$. All the values of δE (mRy) are negative; i.e., the superlattices with mixed interfaces are energetically more stable.
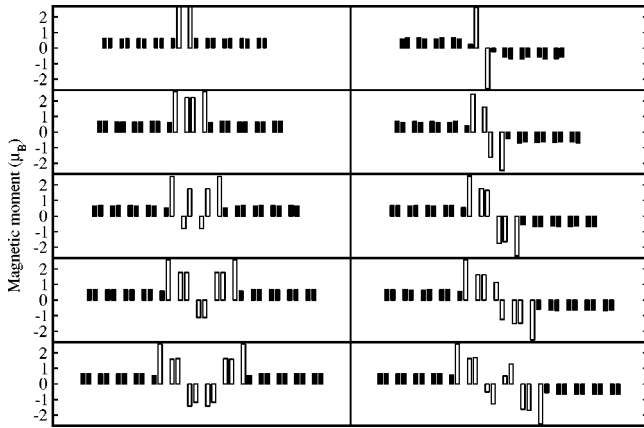
	$n=1$	$n=2$	$n=3$	$n=4$	$n=5$
δE (mRy)	-22	-58	-51	-46	-49

FIG. 6. Magnetic profiles (in μ_B) of $Fe_{n-1}/Ni_{0.5}Fe_{0.5}/Ni_4/Ni_{0.5}Fe_{0.5}$ ($n=1,2,3,4,5$) superlattices for FM and AF interlayer exchange couplings between Ni slabs (left and right panels, respectively); dark and open bars as in Fig. 2.

FIG. 7. The energy differences ($E_F - E_{AF}$) vs the number of Fe layers in the case of $Fe_{n-1}/Ni_{0.5}Fe_{0.5}/Ni_4/Ni_{0.5}Fe_{0.5}$. E_F and E_{AF} as in Fig. 4.

discuss the resulting IEC's in the multilayers with these mixed Ni-Fe interfaces.

The magnetic moments of the Fe atoms in the $Fe_{0.5}Ni_{0.5}$ mixed plane is about $2.6\mu_B$ (Fig. 6). A decrease of the Fe magnetic moment is shown when we go away from Ni similarly to the results already obtained in the case of perfect Fe/Ni interfaces. For a ferromagnetic IEC and for $n=1,2$, the most stable solution is entirely ferromagnetic. The Ni magnetic moment remains close to the bulk value ($0.63\mu_B$). For $n>2$ the most stable solutions display some kind of antiferromagnetism—i.e., $c(2\times2)$ for $n=3$ and layered antiferromagnetism for $n=4$. Let us discuss in more detail the cases $n=3$ and $n=4$ for ferromagnetic IEC between the Ni slabs. For $n=3$ the two Fe layers are clearly of $c(2\times2)$ type and the magnetic moments opposite to the Ni polarization are strongly diminished ($0.8\mu_B$). The Ni atoms in the $Fe_{0.5}Ni_{0.5}$ plane undergo a small diminution of their magnetic moments ($0.51\mu_B$). This decrease arises from the $c(2\times2)$ antiferromagnetic arrangement in the Fe layers. This magnetic behavior is completely different from the corresponding perfect interface for which the $c(2\times2)$ configuration does not exist. For $n=4$ only a layer antiferromagnetic arrangement in the Fe film is obtained. All the nearest Fe atoms surrounding Ni have their moment parallel to the Ni polarization, so that the magnetic moment of Ni of the $Fe_{0.5}Ni_{0.5}$ mixed layer remains equal to $0.59\mu_B$. The magnetic moment of the Fe adjacent planes to the $Fe_{0.5}Ni_{0.5}$ is $1.76\mu_B$ per atom whereas the atoms in the middle plane of the Fe spacer have a magnetic moment of $1.12\mu_B$ opposite to the Ni polarization.

For antiferromagnetic IEC (right panel of Fig. 6) between two adjacent Ni slabs, the Fe film displays always an antiferromagnetic arrangement. Due to this antiferromagnetic order in the Fe spacer, the magnetic moments on the Ni atoms of the $Fe_{0.5}Ni_{0.5}$ plane are depressed. In this $Fe_{0.5}Ni_{0.5}$ mixed plane, the coupling between Ni and Fe is always ferromagnetic with a high Fe moment. For $n=1$, 6 of the 12 nearest neighbors of Ni in the $Fe_{0.5}Ni_{0.5}$ plane are Fe atoms. The polarization of these nearest neighbors is as follows: two Fe
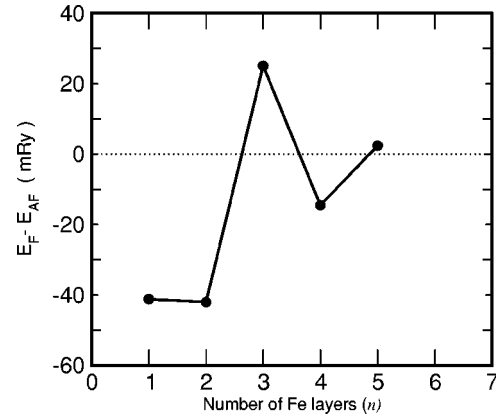
and two Ni atoms have opposite moment to the Ni considered, whereas the rest (four Fe and four Ni) have parallel moments. This magnetic neighborhood leads to a strong diminution of the magnetic moment of the considered Ni atoms of the $Fe_{0.5}Ni_{0.5}$ plane. For $n=2,4$, the more stable state displays a $c(2\times2)$ configuration for the Fe central layer and layer antiferromagnetism for $n=3$. The magnetic moments of the Ni atoms of the mixed plane are $0.42\mu_B$ for $n=2$, $0.55\mu_B$ for $n=3$, and $0.56\mu_B$ for $n=4$ and 5. For $n=3$, the magnetic moments of the two inequivalent atoms of the Fe planes are $1.76\mu_B$ and $1.66\mu_B$. These two atoms have equivalent chemical neighborhoods but different magnetic neighborhoods.

Magnetic moments and energies of transition metals could be quite sensitive to interfacial relaxation especially in the monolayer range. In order to have an idea of the variations of the moments and energies induced by this relaxation, we also fixed the distance at the Ni-Fe interface to that of fcc chemically ordered FeNi. For this compound of $Fe_{0.5}Ni_{0.5}$ stoichiometric, we obtain an equilibrium lattice parameter of 6.70 a.u. However, for this parameter the interfacial Ni-Fe distance increases only of 2% with respect to the mean value $(a_{Fe}+a_{Ni})/2$. In this case the moments and energies do not undergo significant variations.

The interesting point which can be retained for the superlattices with mixed interfaces is the competition between the Fe-Ni ferromagnetic coupling at the interface and the antiferromagnetic coupling between the Fe atoms. As shown in Fig. 6 the magnetic map depends on this competition. One can notice that Fe is not to be considered as a simple spacer since it bears larger magnetic moments than Ni. The coupling between the Ni-Fe mixed plane and the nearest Fe plane is ferromagnetic for the more stable configurations. This can be seen by comparison of the energies of Fig. 7 and the magnetic map reported in Fig. 6. This behavior leads to a completely different magnetic map and oscillatory behavior as that obtained for the superlattices with perfect interface. One can notice, also, that fcc(100) Fe stacked planes could tend to develop noncollinear magnetic ordering due to the geometrical frustration of the AF fcc structure. However, these
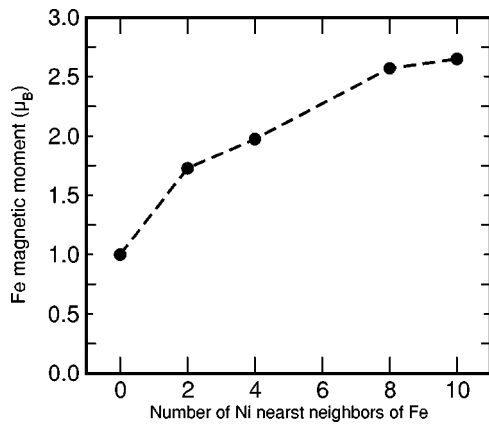
FIG. 8. The Fe magnetic moment as a function of the number of its Ni nearest neighbors.

calculations are beyond the capabilities of the TB-LMTO-ASA method used here.

In Fig. 8 we report the magnetic moment of Fe atoms versus the number of its nearest Ni neighbors. The number of nearest Ni neighbors depends on the position of the Fe atom in the supercell and the value of n. The Fe atoms of the mixed plane have ten foreign Ni nearest neighbors for $n=1$, the corresponding magnetic moment being $2.65\mu_B$, and eight for $n=2,3,4,5$ with, respectively, $2.6\mu_B, 2.56\mu_B, 2.58\mu_B, 2.58\mu_B$ and the mean value is reported in Fig. 8. The atoms of the Fe plane, which is adjacent to the mixed plane, have four foreign Ni nearest neighbors for $n=2$ with $2.21\mu_B$ and two for $n=3,4,5$ with $1.71\mu_B, 1.76\mu_B, 1.66\mu_B$. The mean value is $1.71\mu_B$.

In support of the enhancement of Fe magnetic moment with respect to the fcc bulk value $(1\mu_B)$ even far from the interface, one can consider the experimental studies on Co/Fe multilayers which show that interactions at the Co/Fe interface cause Fe moments enhancements that extend at least 6 ML away from interface.[33]

V. CONCLUSION

We have determined the magnetic map and the interlayer exchange coupling in various fcc Fe/Ni superlattices. The following points are worthy to mention.

(i) The magnetic moment of the Fe atom depends strongly on the number of Ni atoms in its first coordination shell and it goes from a low value of $1.0\mu_B$ for fcc bulk Fe to a very high moment of $2.6\mu_B$ when Fe has ten nearest Ni neighbors (see Fig. 8 for details). This is in agreement with the Mössbauer results of Fratucello et al.[3] displaying a high hyperfine field for Fe atoms close to the Fe-Ni interface with a high-spin ferromagnetic state and a low hyperfine field corresponding to the inside Fe atoms with a low-antiferromagnetic state.

(ii) The Fe-Ni coupling is always ferromagnetic for a perfect interface as well as mixed layer. The iron atoms close to the interface tend to order ferromagnetically whereas the atoms inside the fcc-Fe film give rise to an antiferromagnetic arrangement.

(iii) The in-plane $c(2\times2)$ antiferromagnetic coupling in the Fe layers stabilizes the IEC by minimization of the frustration in the case of an antiferromagnetic IEC in the Fe_n/Ni_m ($n=1,3,5$ and $m=3,5$) superlattices with perfect interfaces and for $n=2,4$ in the case of an ordered mixed layer at the interface of $Fe_{n-1}/Ni_{0.5}Fe_{0.5}/Ni_4/Ni_{0.5}Fe_{0.5}$ superlattices. A $c(2\times2)$ configuration is also obtained in the case of a ferromagnetic IEC for $n=3$ for the superlattices with mixed interface.

(iv) A nonperiodic interlayer exchange coupling between the Ni slabs is found.

(v) Interfacial mixing tends to stabilize the Fe/Ni superlattices and modifies strongly the magnetic map and IEC. This interfacial mixing was detected by LEED, PDMEE,[8] and Mössbauer spectroscopy[9,10] so that we can consider that our calculation which supports this idea is realistic. However, it is not clear if our modeling of the interdiffusion (which is shown to stabilize the Fe/Ni superlattices) is the real ground state. More experimental work is necessary to probe (i) the alloyed Fe-Ni interfaces and (ii) the interlayer exchange coupling.

[1] S.H. Lu, Z.Q. Wang, D. Tian, Y.S. Li, and F. Jona, Surf. Sci. **221**, 35 (1989).

[2] G.C. Gazzadi, P. Luches, S. D'Addato, L. Marassi, R. Capelli, L. Pasquali, S. Valeri, and S. Nannarone, Appl. Surf. Sci. **162-163**, 198 (2000).

[3] G.B. Fratucello, A.M. Prandini, P. Luches, S. D'Addato, A.J. Patchett, and S. Nannarone, J. Magn. Magn. Mater. **210**, 349 (2000).

[4] A.S. Edelstein, C. Kim, S.B. Qadri, K.H. Kim, V. Browning, H.Y. Yu, B. Maruyama, and R.K.E. Verett, Solid State Commun. **76**, 1379 (1990).

[5] W. Kuch and S.S.P. Parkin, J. Magn. Magn. Mater. **184**, 127 (1999).

[6] W. Kuch, J. Giles, F. Offi, S.S. Kang, S. Imada, S. Suga, and J. Kirschner, J. Electron Spectrosc. Relat. Phenom. **109**, 249 (2000).

[7] W.L. O'Brien and B.P. Tonner, Phys. Rev. B **52**, 15 332 (1995).

[8] P. Luches, G.C. Gazzadi, A. di Bona, L. Marassi, S. Valeri, and S. Nannarone, Surf. Sci. **419**, 207 (1999).

[9] G.B. Fratucello and A.M. Prandini, J. Electron Spectrosc. Relat. Phenom. **76**, 665 (1995).

[10] B.R. Acharya, S.N. Piramanayagam, A.K. Nigam, S.N. Shringi,

Shiva Prasad, N. Venkataramani, Girish Chandra, and R. Krishnan, J. Magn. Magn. Mater. **140-144**, 555 (1995).

[11] C.E. Johnson, M.S. Ridout, and T.E. Cranshaw, Proc. Phys. Soc. London **81**, 079 (1963).

[12] B.K. Rao, S. Ramos de Debiaggi, and P. Jena, Phys. Rev. B **64**, 024418 (2001).

[13] C.S. Wang, B.M. Klein, and H. Krakauer, Phys. Rev. Lett. **54**, 1852 (1985).

[14] B. M'Passi-Mabiala, S. Meza-Aguilar, and C. Demangeat, Phys. Rev. B **65**, 012414 (2001).

[15] S. Meza-Aguilar, O. Elmouhssine, H. Dreyssé, and C. Demangeat, Phys. Rev. B **63**, 064421 (2001).

[16] V.L. Moruzzi, P.M. Marcus, and J. Kübler, Phys. Rev. B **39**, 6957 (1989).

[17] O.K. Andersen and O. Jepsen, Phys. Rev. Lett. **53**, 2571 (1984).

[18] O.K. Andersen, Z. Pawlowska, and O. Jepsen, Phys. Rev. B **34**, 5253 (1986).

[19] U. Von Barth and L. Hedin, J. Phys. C **5**, 1629 (1972).

[20] P. Hohenberg and W. Kohn, Phys. Rev. B **136**, B864 (1964).

[21] W. Kohn and L.J. Sham, Phys. Rev. A **140**, A1133 (1965).

[22] D.C. Langreth and M.J. Mehl, Phys. Rev. Lett. **47**, 446 (1981).

[23] J.P. Perdew, Y. Wang, and E. Engel, Phys. Rev. Lett. **66**, 508 (1991).

[24] H.C. Herper, E. Hoffmann, and P. Entel, Phys. Rev. B **60**, 3839 (1999).

[25] L. Kleinman, Phys. Rev. B **59**, 3314 (1999).

[26] E.G. Moroni, G. Kresse, J. Hafner, and J. Furthmüller, Phys. Rev. B **56**, 15 629 (1997).

[27] H.J.F. Jansen and S.S. Peng, Phys. Rev. B **37**, 2689 (1988).

[28] P.M. Marcus, V.L. Moruzzi, and S.-L. Qiu, Phys. Rev. B **60**, 369 (1999).

[29] K. Knöpfle, L.M. Sandratskii, and J. Kübler, Phys. Rev. B **62**, 5564 (2000).

[30] D.J. Singh and J. Ashkenazi, Phys. Rev. B **46**, 11 570 (1993).

[31] M. Methfessel, C.O. Rodriguez, and O.K. Andersen, Phys. Rev. B **40**, 2009 (1989).

[32] T. Veres, M. Cai, R.W. Cochrane, M. Rouabhi, S. Roorda, and P. Desjardins, Thin Solid Films **382**, 172 (2001).

[33] S. Pizzini, A. Fontaine, E. Dartyge, C. Giorgetti, F. Baudelet, J.P. Kappler, P. Boher, and F. Giron, Phys. Rev. B **50**, 3779 (1994).